Circadian Disruption Exacerbates Innate Immune Responses by Modulating the Bistability of Pro-Inflammatory Signaling: A dynamical Modeling Study

Quan Zhou , Qi Ouyang , Hongli Wang *

Posted Date: 2 June 2026

doi: 10.20944/preprints202606.0096.v1

Keywords: circadian clock; innate immunity; mathematical model; inflammation; bistability

 doi:10.20944/preprints202606.0096.v1

Article

Circadian Disruption Exacerbates Innate Immune Responses by Modulating the Bistability of Pro-Inflammatory Signaling: A dynamical Modeling Study

Quan Zhou [1], Qi Ouyang [2] and Hongli Wang [1,3,*]

[1] The State Key Laboratory for Artificial Microstructures and Mesoscopic Physics, School of Physics, Peking University, Beijing, China

[2] School of Physics, Zhejiang University, Hangzhou, China

[3] Center for Quantitative Biology, Peking University, Beijing, China

* Correspondence: hlwang@pku.edu.cn

Abstract

Circadian disruption resulting from factors such as jet lag, shift work, or aging leads to exaggerated inflammatory responses and increased disease susceptibility. However, the core dynamical mechanism by which circadian disruption exacerbates innate immune responses remains poorly understood. Here, we develop an integrated mathematical model coupling the mammalian circadian clock with antigen-induced innate immune responses, incorporating key regulatory interactions including glucocorticoid modulation and pro-inflammatory positive feedback loops. The model successfully recapitulates experimental data regarding homeostatic immune circadian oscillations and time-dependent gating of acute inflammatory responses. Dynamic analyses reveal that the circadian clock exerts its gating function by modulating the bistable characteristics within pro-inflammatory positive feedback loops. Circadian disruption, simulated as jet lag or age-related reduction in clock gene amplitude, reshapes this bistable landscape and prolongs residence duration in the pathological hyperinflammatory state. This shift not only amplifies acute cytokine bursts but also sustains exaggerated inflammatory activity, providing a unifying mechanistic explanation for acute tissue injury and chronic low-grade inflammation (inflammaging) under circadian disruption.

Keywords: circadian clock; innate immunity; mathematical model; inflammation; bistability

1. Introduction

The circadian clock is an endogenous timing system that entrains to the day–night cycle, periodically regulating immune function [1,2]. This regulation is mediated by transcription–translation feedback loops (TTFLs) with ~24-hour periods, which constitute the core clock mechanism across taxa from fungi to mammals [3] and regulate diverse physiological processes [4]. In the context of immunology in mammals, the circadian gating of innate immunity is particularly critical. The clock modulates bone-marrow homing and peripheral egress by tuning chemokine and receptor expression [5–8]. In parallel, the circadian system gates the activity of immune cells [9,10], cytokines [11,12], certain receptors [13], and the complement system [14], causing these immune components to oscillate with a near 24-hour period. More importantly, cytokine sensitivity to stimulation varies with time of day [11,15], further demonstrating the time dependence of innate immune components under circadian control. Complementing these local mechanisms, the circadian system also exerts systemic control via the hypothalamic-pituitary-adrenal (HPA) axis. The rhythmic secretion of glucocorticoids (CORT), which peaks during the active phase [16], functions mainly as a potent systemic immunomodulatory 'brake' that sets the threshold for pro-inflammatory cytokines and coordinates with local molecular clocks [17–19].

 doi:10.20944/preprints202606.0096.v1

In recent decades, accumulating evidence has linked circadian **abnormality** to the pathogenesis of various diseases. Factors such as unhealthy lifestyle factors [20], disease [21], disrupted light–dark cycle [22], or aging [23] can lead to circadian misalignment or reduced clock gene amplitude, exacerbating various diseases, including Parkinson's disease [24], depression [25], Alzheimer's disease [26], and atherosclerosis [27]. Among these, the most direct effect of circadian disruption on the immune system is a significant exaggeration of the host innate immune response to external inflammatory stimuli. Animal experiments using mice subjected to serial advances of the light-dark cycle (chronic jet lag, CJL) showed dysregulation of core and peripheral clock genes, leading to altered cytokine release [28,29], and a markedly higher mortality rate after endotoxin challenge (89% vs. 21% in controls) [30]. Studies in rodent shift-work models and workers with chronic shift-work schedules have shown that circadian disruption not only increases the host susceptibility to acute stimuli [31] but also induces persistent low-grade inflammation, as evidenced by significantly elevated concentrations of plasma inflammatory markers and cytokines [32]. Experiments exposing mice to light at night have similarly reported dysregulated cytokine release and responses, as well as anxiety- and depression-like behaviors [25]. Aging is often accompanied by a decrease in the amplitude of core clock gene expression [23], heightening innate responses to stimuli and increasing both acute responses to endotoxin (vs. young mice) and the risk of chronic inflammation [33,34]. Of particular note, extreme circumstances such as sleep deprivation can even induce cytokine storm, leading to uncontrolled elevations of pro-inflammatory cytokines, multiple organ dysfunction syndrome, and even death [35]. Collectively, these studies establish the circadian clock as an inhibitory gatekeeper essential for innate immune homeostasis and provide a foundation for developing integrated dynamic models to dissect its underlying mechanisms.

How circadian dysfunction disrupts this gatekeeper role and drives excessive inflammatory immune reactions is a compelling open question in circadian–immune interaction research. **To address such complex, systems-level question, mathematical modeling has become an indispensable tool.** The dynamics of immune responses are increasingly analyzed using complex networks that integrate processes such as genetic regulation, cytokine secretion, and leukocyte trafficking. Foundational work in this area includes mathematical models of the acute inflammatory response to endotoxin challenges, which provided frameworks for understanding the balance between pro- and anti-inflammatory signaling [36,37]. The approach has been extended to infectious disease. For instance, a recent multicompartment model of host immunity successfully addressed the heterogeneity of COVID-19 clinical presentations by integrating lymphocyte and cytokine trafficking [38]. Furthermore, Zhou et al. introduced a predictive metric termed "immune efficacy" to forecast SARS-CoV-2 outcomes, demonstrating the clinical utility of such models. Building on these advances, researchers have recently focused on modeling the specific influence of circadian rhythms on immunity. For example, sexually dimorphic effects of shift work were investigated using a model of circadian-immune regulation in rats [39], revealing that circadian timing modulates sex-specific cytokine responses. At the systems level, Balit et al. [40] integrated circadian rhythms with $CD8^+$ T cell dynamics, finding that a bistable signaling switch enables circadian forcing to generate day–night differences in T cell activation. Most recently, efforts have focused on the time-of-day dependence of viral exposure and vaccination [41]. **Critically, these latest studies are beginning to uncover the specific mechanisms hidden in the complex circadian regulated immunity.** They demonstrated that the clock-controlled release of CCL2 in the innate immune response, or the circadian regulation of antigen-presenting cells, directly determines the time-of-day-dependent immune response. These findings suggest that circadian disruption may exacerbate immune responses precisely by perturbing these identified gatekeeping processes.

The purpose of this paper is to construct a comprehensive model of the circadian clock-innate immune response to quantitatively elucidate the core dynamic mechanism by which circadian **abnormality** regulates exaggerated inflammatory responses. The model for mammals integrates currently known interactions between the circadian clock and innate immunity and considers the effects of two typical circadian disruptors, *i.e.*, jet lag and aging, on innate immune dynamics.

 doi:10.20944/preprints202606.0096.v1

Simulations of our model successfully reproduce experimentally observed circadian oscillations and time-dependent inflammatory responses. Dynamic analyses reveal that distorted circadian oscillations induced by jet lag or aging reshape the bistable landscape of a pro-inflammatory positive feedback loop. This reshaping both amplifies acute cytokine responses and prolongs residence time in a high-inflammation state, thereby sustaining exaggerated inflammatory activity. This provides a unifying explanation for chronic low-grade inflammation under abnormal circadian conditions. These mechanistic insights offer a theoretical framework for understanding the origins of chronic inflammation (such as inflammaging) and provide a foundation for the precise control of immune-mediated tissue damage and the development of chronotherapies for diseases associated with circadian rhythm disorders.

2. Materials and Methods

2.1. Network of Circadian-Regulated Innate Immune Responses

In mammals, the innate immunity is the first line of fast defense against pathogens and provides fundamental and comprehensive protection. The core components of innate immunity are closely regulated by the circadian clock, particularly in rhythmic release of innate immune cells from the bone marrow, the rhythmic secretion of cytokines in tissues, and immune response in peripheral tissues to antigen stimulation. Here, we construct a mathematical model of circadian clock-regulated innate immunity, with the aim to quantitatively investigate the effect of clock disruption caused by jet-lag or aging on inflammatory responses due to antigen (such as lipopolysaccharide (LPS)) stimulation. As depicted in Figure 1, the multicompartmental model integrates peripheral tissue, peripheral blood, and bone marrow, which are all regulated by the circadian clock.

The construction of the core circadian clock in our model adheres to the central TTFL molecular mechanism of the mammalian circadian clock (see Figure 1, the module shown in light blue) [3]. In the TTFL, transcription factors BMAL1 and CLOCK first form a heterodimer, binding to E-box elements in the promoter regions of *PER* and *CRY* genes to promote their transcription and translation. Subsequently, PER and CRY proteins form a dimer, enter the nucleus, and inhibit CLOCK-BMAL1 activity by directly binding to the complex, forming the core negative feedback loop. In addition, REV-ERB and ROR proteins constitute secondary feedback loops by binding to the ROR response elements (RORE) of the *BMAL1* gene, respectively repressing and activating *BMAL1* transcription, thereby stabilizing circadian oscillations. In the circadian clock module, the subtypes of various genes (such as *PER*/*CRY*/*REV-ERB*/*ROR*) are limped together, and CLOCK protein is assumed to be stably expressed [42]. In our model, the circadian clock is shared across the compartments of peripheral tissue, blood, and bone marrow.

 doi:10.20944/preprints202606.0096.v1

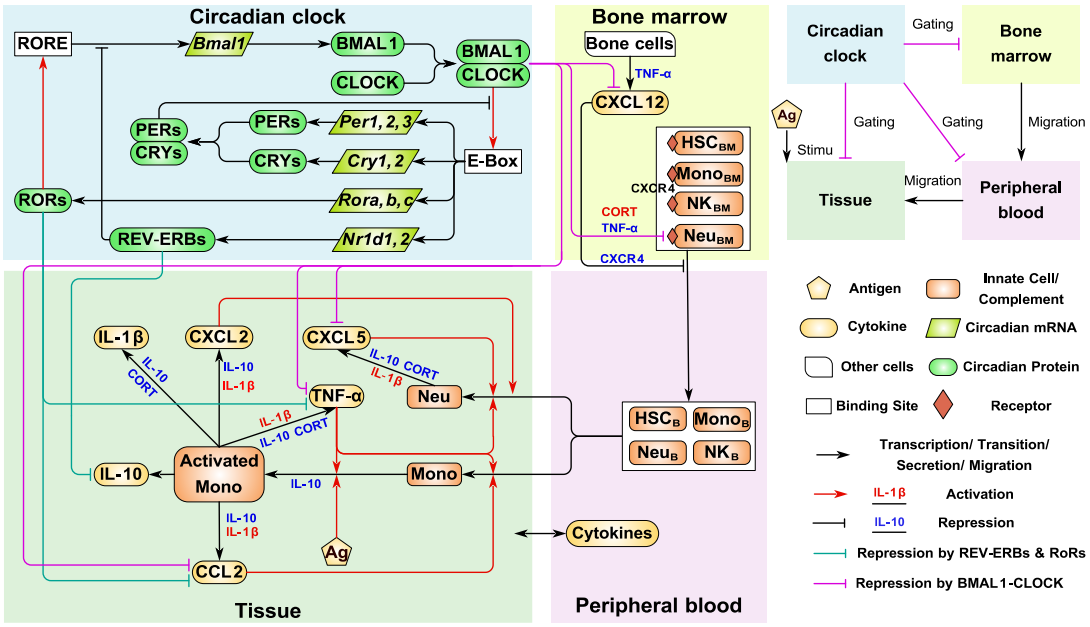

Figure 1. Schematic of the circadian regulation of the innate immune response. Modules are color-coded: light blue represents the canonical TTFL circadian clock, yellow the bone marrow, green the peripheral tissue where innate immunity is activated, and light red the peripheral blood. Circadian clock proteins, including BMAL1, CLOCK, PERs, CRYs, RORs, and REV-ERBs, are depicted as green rounded rectangles. Immune cells, comprising monocytes/macrophages, neutrophils, natural killer cells, and hematopoietic stem cells, are shown as brown rounded rectangles and labeled with the abbreviations Mono, Neu, NK, and HSC, respectively. The immune cells released from the bone marrow circulate in the peripheral blood, where they are recruited or activated by cytokines before entering tissues to participate in the innate immune response. Cytokines are represented by yellow rounded rectangles, with CCL2, IL-1β, TNF-α, IL-10, and CXCL5 exchanged between peripheral tissue and blood. The circadian regulation from the HPA axis is incorporated by introducing the glucocorticoids which is abbreviated as CORT. The upper-right block summarizes the interactions among the four modules.

In peripheral tissue, the core mechanisms of acute innate immune response is represented by the compartment in light green in Figure 1 [43]. Upon stimulation by an external antigen (Ag in Figure 1), local monocytes/macrophages (represented with Mono in Figure 1) become activated. The activation of monocytes/macrophages rapidly secrets pro-inflammatory cytokines such as tumor Necrosis Factor-α (TNF-α), interleukin-1β (IL-1β) and C-C motif chemokine ligand 2 (CCL2). TNF-α also reinforces local monocytes/macrophages activation, forming a positive feedback loop that amplifies the inflammatory response. Concurrently, to prevent excessive inflammatory activation, the activated monocytes/macrophages secrete the anti-inflammatory factor Interleukin-10 (IL-10), which constitutes a self-limiting regulation by suppressing macrophage activation to reduce cytokine secretion. Additionally, activated monocytes/macrophages secrete the neutrophil-recruiting chemokine C-X-C motif chemokine ligand 2 (CXCL2), which, together with TNF-α, promotes neutrophil (Neu in Figure 1) recruitment from peripheral blood into the stimulated tissue. Neutrophils, after entering the tissue, also secrete C-X-C motif chemokine ligand 5 (CXCL5), which further reinforces neutrophil recruitment in the tissue compartment.

In the peripheral blood compartment (Figure 1, light red module), the cytokines (excluding CXCL2) are represented by a lumped "Cytokines" node. The bidirectional connection between the blood "Cytokines" node and the tissue compartment represents the exchange of these cytokines between blood and tissue. The innate immune cells in blood, such as neutrophils, monocytes, natural killer cells, and hematopoietic stem cells, are released from the bone marrow (Figure 1, light yellow

 doi:10.20944/preprints202606.0096.v1

module). The release process is regulated by the CXCL12–CXCR4 axis: CXCL12 in the bone marrow binds to C-X-C chemokine receptor 4 (CXCR4) on immune cells and thereby inhibits their release from the bone marrow [44,45].This joint retention effect is represented in Figure 1 by an inhibitory link from CXCL12, with CXCR4 indicated as a co-mediating factor. Under inflammatory conditions, this retention effect is weakened, allowing increased release of innate immune cells into the circulation. This is modeled by allowing TNF-α to inhibit both CXCL12 and CXCR4, consistent with the reported TNF-α-dependent reduction of CXCL12 [46]. To simplify the model, the homing process of immune cells is not explicitly considered [47]. Instead, this process is absorbed into the cell loss term, such that the corresponding coefficient represents an effective removal rate rather than a pure intrinsic decay rate.

In Figure 1, the regulation of immunity by the circadian clock is depicted via links connecting clock proteins to target nodes within the immune system. In the tissue compartment, CLOCK-BMAL1 represses the syntheses of CCL2 [12,48], TNF-α [39,49], CXCL5 [17]. RORs inhibit the production of CCL2 [12,48], TNF-α [39,49]. In the bone marrow compartment, CLOCK-BMAL1 inhibits the production of CXCL12 [7] and CXCR4 [6], rhythmically regulating the release of innate immune cells from bone marrow to peripheral blood [8]. To incorporate the circadian regulation by the HPA axis, we also introduced CORT as a key inhibitor in the innate immune system. CORT downregulates the secretion of pro-inflammatory cytokines (TNF-α, IL-1β) and the chemokine CXCL5, reflecting its well-documented immunosuppressive effects [17–19]. In addition, CORT is modeled as a positive regulator of CXCR4, thereby reinforcing the retention axis and contributing to circadian control of leukocyte trafficking [50]. These regulatory pathways enable the system to reproduce the 24-hour oscillation of innate immune components and provide a systems-level basis for analyzing the mechanisms of dysregulated immune response under circadian disruption.

2.2. Equations

The circadian regulation of innate immune dynamics shown in Figure 1 is described mathematically by a set of coupled nonlinear ordinary differential equations (ODEs) (see Eqs. S1–S34 and Table S1 for the ODEs and dynamic variables in Supplementary Materials). These ODEs describe key physiological processes within the system—including cell release, transformation, and recruitment; cytokine secretion, diffusion, and degradation; receptor expression and regulation—as well as the cross-regulation among these processes. Together, they constitute a comprehensive dynamic modeling framework for innate immunity under circadian control. Hill functions have been extensively used. For example, if secretion of the cytokine TNF-$\boldsymbol{\alpha}$ is simultaneously inhibited by the anti-inflammatory factor IL-10, this is represented as a modulatory term in the secretion rate of TNF-$\boldsymbol{\alpha}$ of the form $\frac{K_{\mathrm{IL10\_TNF\alpha}}^2}{K_{\mathrm{IL10\_TNF\alpha}}^2+[\mathrm{IL10}]^2}$ (see Eq. S27 in Supplementary Materials). For inter-compartmental cell migration processes in our model, such as the recruitment of neutrophils from blood into infected peripheral tissue, cells are recruited by the chemokine CXCL5 and depend on endothelial permeability (modulated by TNF-α), which results in an influx rate proportional to the product of these regulatory terms of the form $\frac{c_{\mathrm{CXCL5\_Neu}}\cdot[\mathrm{CXCL5}]^2}{K_{\mathrm{CXCL5\_Neu}}^2+[\mathrm{CXCL5}]^2}\cdot\left(1+\frac{h_{\mathrm{TNF\alpha\_Neu}}\cdot[\mathrm{TNF\alpha}]}{K_{\mathrm{TNF\alpha\_Neu}}+[\mathrm{TNF\alpha}]}\right)$ (see Eq. S14 in Supplementary Materials). For cytokines diffusing between blood and peripheral tissue, the diffusion rates are determined by the concentration difference between the two sides. Take IL-10 for an instance (see Eq. S20 in Supplementary Materials), the net inflow to tissue is proportional to $[\mathrm{IL10Blood}]/\boldsymbol{k_{Blood}}-[\mathrm{IL10}]$, and the net inflow to blood is proportional to $[\mathrm{IL10Blood}]-\boldsymbol{k_{Blood}}[\mathrm{IL10}]$, where $\boldsymbol{k_{Blood}}$ is estimated from the volume ratio between peripheral tissue (taking the peritoneal cavity as an example) and blood. The dynamic description for the module of TTFL circadian clock follows the approach of Wei et al. [42], with key parameters adjusted to capture the experimental observations of circadian clock abnormalities induced by jet lag and aging [22,23]. The diurnal oscillation of CORT at homeostasis is modeled by a non-autonomous ODE with a 24-hour sinusoidal driving term (see Eq. S34 in the Supplementary Materials). Upon endotoxin stimulation,

 doi:10.20944/preprints202606.0096.v1

the acute elevation of CORT is modeled by introducing an additional time-dependent pulse term into the rate equation for CORT, which fits the experimental data of post-endotoxin serum profiles [51] (see Eq. S34 in Supplementary Materials). The inhibitory effect of CORT on cytokine secretion (such as TNF-α, IL-1β, CXCL5) is represented by Hill-type inhibitory functions (e.g., $\frac{K_{CORT\_TNFa}^{n}}{K_{CORT\_TNFa}^{n} + [CORT]^{n}}$) (see Eq. S27 in Supplementary Materials). In our model, the circadian signal that regulates immunity is assumed to originate from peripheral clocks located in tissues, blood, and bone marrow. These peripheral clocks generate a unified circadian rhythmicity that is synchronized by the master clock in the brain's suprachiasmatic nucleus, under both normal and abnormal conditions such as jet lag and aging. Normal and abnormal circadian rhythmicity are distinguished by the parameter values within the circadian clock module, and the same holds for CORT rhythmicity. Independently of the circadian clock, the structure and parameters of the immune module, together with the parameters governing clock/CORT-to-immunity coupling, are held constant. In this paper, the ODEs are solved numerically in MATLAB using the stiff solver ode15s, with the parameter values given in the Supplementary Materials.

2.3. Parameter Estimation

The ODE model contains 34 state variables and 152 parameters. Of these parameters, 53 are related to the circadian clock, 7 to circadian rhythms of corticosterone (CORT), and 92 to innate immunity. The detailed parameter classifications and numerical values are summarized in Supplementary Tables S2–S6. These parameter values are determined through multiple approaches: inferred from reported experimental measurements, estimated according to physiological ranges, adopted from existing mathematical models, and derived from experimental data fitting. The detailed fitting approach and objective functions are described in Supplementary section 'S3. Parameter fitting'. Parameter determination and fitting adopt a multi-stage strategy, proceeding from upstream circadian clock to downstream innate immunity. For the normal circadian clock, the 53 parameters of the upstream clock module are adopted from existing models [39,42] to reproduce the normal circadian rhythm [52] (see Supplementary Table S2). A subset of parameters (Supplementary Table S3) are adjusted to capture the altered circadian rhythms under jet-lagged and aged conditions [22,23]. In parallel, 7 CORT-related parameters (Supplementary Table S4) are fitted to basal CORT profiles under normal, jet-lagged, and aging conditions, together with LPS-induced acute CORT responses [16,53]. Of the 92 innate immune parameters (see Supplementary Tables S5–S6), 11 are experimentally inferred, 6 are estimated under physiological constraints, and 4 are adopted from existing mathematical models. The remaining 71 innate immune parameters are derived from data fitting. Under unstimulated steady-state conditions, the innate immune system downstream from the circadian clock displays a basal circadian rhythm. As cytokine concentrations remain at low levels with minimal mutual interaction, the components of the system are weakly coupled. This modularity enables a subset of parameters governing circadian rhythms to be fitted largely independently [20,54,55] (Supplementary Table S5). The fitted experimental data include: circadian rhythms in CXCL12 and CXCR4 [7,8]; circadian rhythms of circulating neutrophils, monocytes, NK cells, and HSCs [8]; the coupled rhythms of tissue monocytes and blood CCL2 [20,54]; and finally, the peak-normalized basal TNF-α rhythmic profile [55]. The remaining innate immune parameters are associated with acute immune responses to antigen stimulation, which are derived by fitting to LPS-stimulated experimental datasets (Supplementary Table S6). These parameters are determined in two steps. We first calibrate the core upstream cytokines of TNF-α, IL-1β, and IL-10 using time-of-day-dependent IL-1β and IL-10 data [15] (see Supplementary Figure S2), along with TNF-α, IL-1β, and IL-1β measurements under jet-lagged and aged conditions. Relevant datasets are also extracted from those published studies under the normal circadian clock regulation [30,33]. The remaining unresolved parameters associated with downstream CCL2 and CXCL5 responses are estimated using their time-of-day-dependent stimulation data [15].

 doi:10.20944/preprints202606.0096.v1

We carried out sensitivity and identifiability analyses for the 71 fitted parameters associated with innate immunity, with results shown in Supplementary Figures S3 and S4-S6 (see also Supplementary S4. Sensitivity Analysis and Parameter Identifiability). Among the top 20 most sensitive parameters, the majority are linked to monocyte (Mono) activation, particularly Ag/AR-related ones including $K_{\mathrm{Ag\_AR}}, c_{\mathrm{Ag\_AR}}$, $K_{\mathrm{IL10\_Ag}}$, d_{Ag}, d_{AR}, and d_{Mono}. As monocyte activation acts upstream of immune responses and controls most cytokine secretion, these parameters are highly sensitive. High-ranking parameters also cover core pro-inflammatory cytokines CCL2 and TNFα, represented by $c_{\mathrm{CCL2\_Mono}}$, t_{CCL2}, d_{CCL2}, $K_{\mathrm{CCL2\_Mono}}$, $K_{\mathrm{Mono\_TNFa}}$, $K_{\mathrm{BC\_TNFa}}$, $K_{\mathrm{ROR\_TNFa}}$, and $K_{\mathrm{Mono\_Il1b}}$. Anti-inflammatory IL-10-related parameters $K_{\mathrm{Mono\_IL10}}$, d_{IL10}, and t_{IL10}. also rank highly, as IL-10 negative feedback closely interacts with monocyte-mediated positive feedback loops and strongly shapes stimulus-induced peak responses. Moreover, K_{BT} mediates cytokine diffusion and trafficking between tissues and blood, and c_{CXCR4} modulates cellular circadian rhythms, explaining their considerable parameter sensitivity. Among the 34 parameters regulating weak oscillations under antigen-free conditions, six are non-identifiable and predominantly associated with CXCL12, including, including $K_{\mathrm{CXCL12\_Neu}}, K_{\mathrm{CXCL12\_NK}}$, and $K_{\mathrm{CXCL12\_Mono}}$. Of the remaining 37 parameters linked to antigen-induced responses, 15 are non-identifiable; these primarily control CXCL5-mediated neutrophil recruitment, such as $c_{\mathrm{Neu\_CXCL5}}$, $c_{\mathrm{CXCL5\_Neu}}$, $K_{\mathrm{CXCL5\_Neu}}$, $h_{\mathrm{IL1b\_CXCL5}}$, d_{CXCL5},$h_{\mathrm{TNFa\_Neu}}$, $K_{\mathrm{TNFa\_Neu}}$ and d_{Neu}.

3. Results

3.1. Homeostatic Circadian Rhythms Under The Regulation of Normal, Jet-Lagged, and Aged Circadian Clocks

In our model, the oscillation dynamics of the upstream circadian clock can be simulated independently, as it regulates innate immunity and is not subject to feedback from the downstream innate immune system. Figure 2 depicts the simulation results of normal circadian rhythmicity and disrupted circadian oscillations induced by jet lag and aging, in comparison with experimental data from mice. The mRNA expression levels of four core clock genes, i.e., *Per*, *Cry*, *Nr1d1*, and *Bmal1*, are shown in Figure 2A–D. Jet lag induced by a phase-advanced light cycle in mice produces circadian oscillations with a 4–6 hour phase shift and decreased oscillation amplitude [22]. In aged mice, the oscillation amplitude is also markedly reduced [23]. While the period of circadian oscillations remains largely unchanged, the mean level of these oscillations is significantly reduced under both jet-lagged and aged conditions compared to that of the normal circadian clock. The simulations agree well with experimental data, accurately capturing the experimentally observed reductions in amplitude and mean value, as well as phase shifts. The comparison between the circadian oscillations of normal circadian clock proteins and the aberrant oscillations induced by shift work and aging is shown in Figure 2F–H. Simulation results for protein levels again demonstrate that both the amplitude and mean level of circadian oscillations are consistently reduced under these circadian disruptions. Compared with the normal clock, the amplitudes of core clock proteins such as PERs, CRYs, and REV-ERBs (Figure 2F), RORs (Figure 2G), and CLOCK-BMAL1 (Figure 2H) are reduced in the disrupted circadian clocks. Notably, the jet-lagged clock exhibits a clear phase shift in the CLOCK-BMAL1 complex, while the aging clock is characterized by a marked suppression of amplitude across all core proteins. These simulated protein-level alterations are consistent with experimentally observed changes under clock disruptions [56,57]. As depicted in Figure 2E, the influence of jet lag and aging on the core circadian clock is also observed in the oscillations of corticosterone in the HPA axis. The simulation of dynamic changes in CORT accurately reproduces the physiological circadian rhythm, characterized by a peak concentration at ZT12 under normal conditions, with a similarly reduced amplitude and mean level in aged and jet-lagged mice and a delayed phase in the case of jet lag as observed in experiments [16,53]. Also, the model successfully reproduces the rapid CORT surge following LPS challenge under the normal situation as in experiment [51] (see Supplementary Figure).

 doi:10.20944/preprints202606.0096.v1

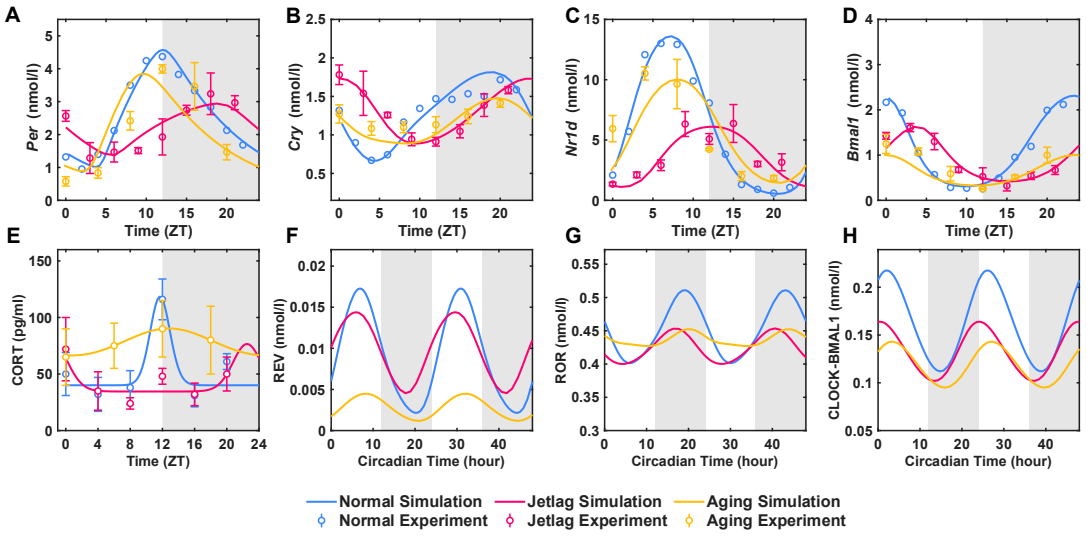

Figure 2. Circadian clock oscillations under normal, jet-lagged, and aged conditions. (A–D) Circadian rhythms in mRNA levels of four core clock genes under normal (blue), jet-lagged (magenta), and aged (yellow) conditions: (A) Per, (B) Cry, (C) Nr1d, and (D) Bmal1. Lines represent simulation results, and circles denote experimental data [22,23,52]. (E) Diurnal oscillations of basal plasma CORT levels under normal, jet-lagged, and aged circadian clocks. The normal rhythm peaks at ZT12, whereas disrupted clocks exhibit dampened amplitudes and altered baselines. Lines represent simulation results, and circles denote experimental data [16,53]. (F–H) Simulated circadian oscillations in core clock proteins under normal, jet-lagged, and aged conditions over a 48-h period: (F) REV-ERB (REV), (G) ROR, and (H) CLOCK-BMAL1 protein complex.

 doi:10.20944/preprints202606.0096.v1

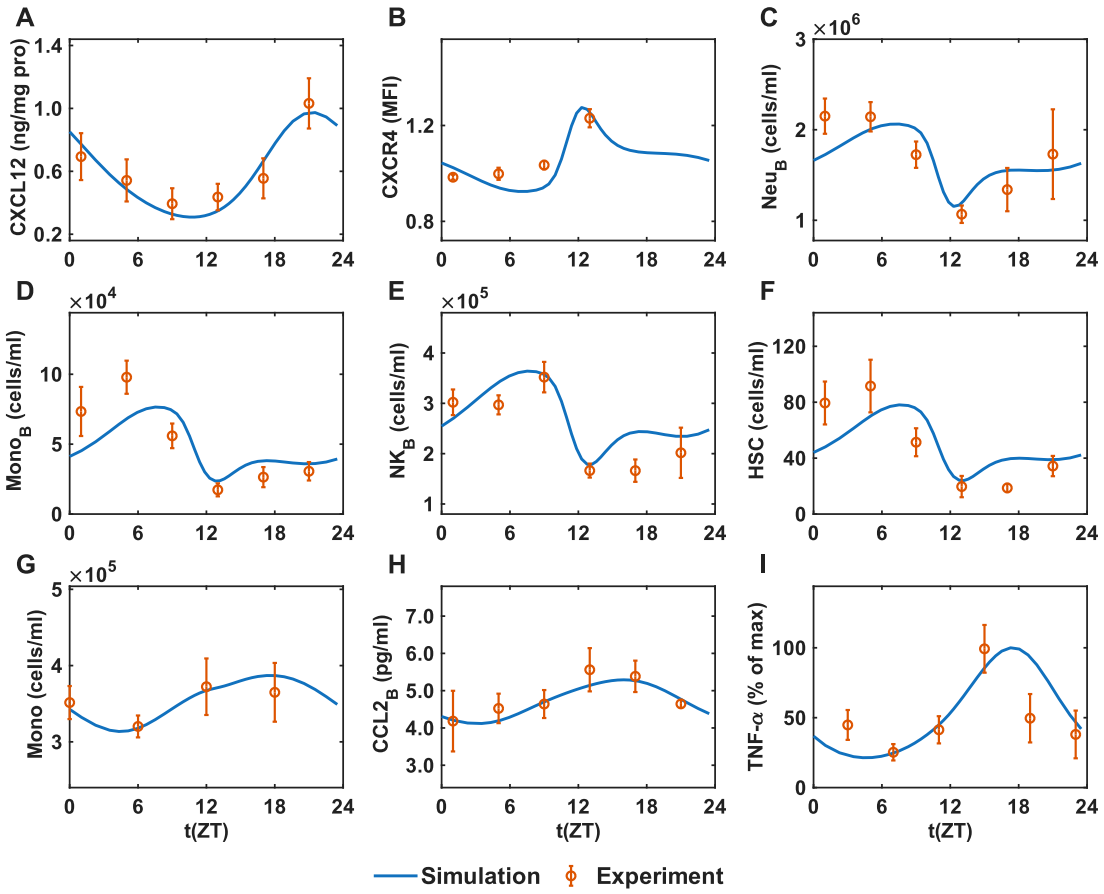

Figure 3. Simulated diurnal oscillations of immune-cell abundance and cytokines regulated by the normal circadian clock under homeostasis without antigen stimulation, compared with experimental data. (A) bone marrow CXCL12 levels; (B) cell-surface CXCR4 expression; (C) peripheral blood neutrophil counts (Neu_B); (D) peripheral blood monocyte counts (Mono_B); (E) peripheral blood natural killer cell counts (NK_B); (F) circulating hematopoietic stem cell counts (HSC); (G) tissue monocyte counts; (H) plasma CCL2 concentration; and (I) tissue TNF-α levels. Blue lines represent simulation results, and orange circles denote experimental data [7,8,20,54,55].

In healthy mammals at homeostasis, the endogenous circadian clock governs robust 24-hour rhythms in the abundance and migration of innate immune cells, along with the expression and activity of innate immune receptors, cytokines, and signaling molecules. We next simulated the rhythmicity of innate immunity under homeostatic conditions, regulated by the normal circadian clock oscillations (see Figure 2). Figure 3 depicts the simulated circadian rhythms in the innate immune system, in the absence of infection or other stimuli, in comparison with experimental measurements in mice. The model reproduced the circadian circulation of innate immune cells, showing overall agreement with experimental data [7,8]: circulating neutrophils (Figure 3C), monocytes (Figure 3D), NK cells (Figure 3E), and hematopoietic stem cells (HSC) (Figure 3F) in peripheral blood, peaking around ZT6. CXCL12 concentration in the bone marrow peaks near ZT22 (Figure 3A), exhibiting an antiphase relationship with immune-cell counts in the blood, while cell-surface CXCR4 peaks around ZT12 (Figure 3B). In addition to cellular rhythms, the model's simulations of oscillations in key immune molecules are consistent with experimental findings: Peripheral tissue monocyte concentration peaks at ZT12–18 (Figure 3G) [20], plasma CCL2 at ZT13–17 (Figure 3H) [54], and tissue TNF-α at ZT15–18 (Figure 3I) [55].

 doi:10.20944/preprints202606.0096.v1

We further simulated the homeostatic dynamics of the innate immune system under the regulation of a jet-lagged or aged circadian clock. Figure 4 presents the simulation results of diurnal oscillations in immune cells and inflammatory cytokines without antigen stimulation, in comparison with the circadian oscillations simulated under the regulation of a normal circadian clock. For the circadian rhythms of circulating cell counts (Figure 4A–C), the simulation results show that abnormal circadian clocks attenuate their diurnal oscillation amplitudes. This trend is qualitatively consistent with the findings reported by Zhao et al., who observed disrupted circadian rhythms of circulating leukocytes in mice [58]. For tissue-resident cells (Figure 4D), experimental evidence has shown that tissue monocyte concentrations are elevated in aged mice across multiple peripheral tissues [59], which is also consistent with the simulation results. Finally, for cytokine concentrations (Figure 4E–F), existing studies have demonstrated that mice subjected to chronic jet lag exhibit elevated serum TNF-α levels under unstimulated conditions [60], while immune cells from aged mice show higher expression of inflammatory cytokines without LPS stimulation [59]. These findings are qualitatively consistent with the model-predicted elevation of basal inflammatory levels under abnormal circadian clock conditions.

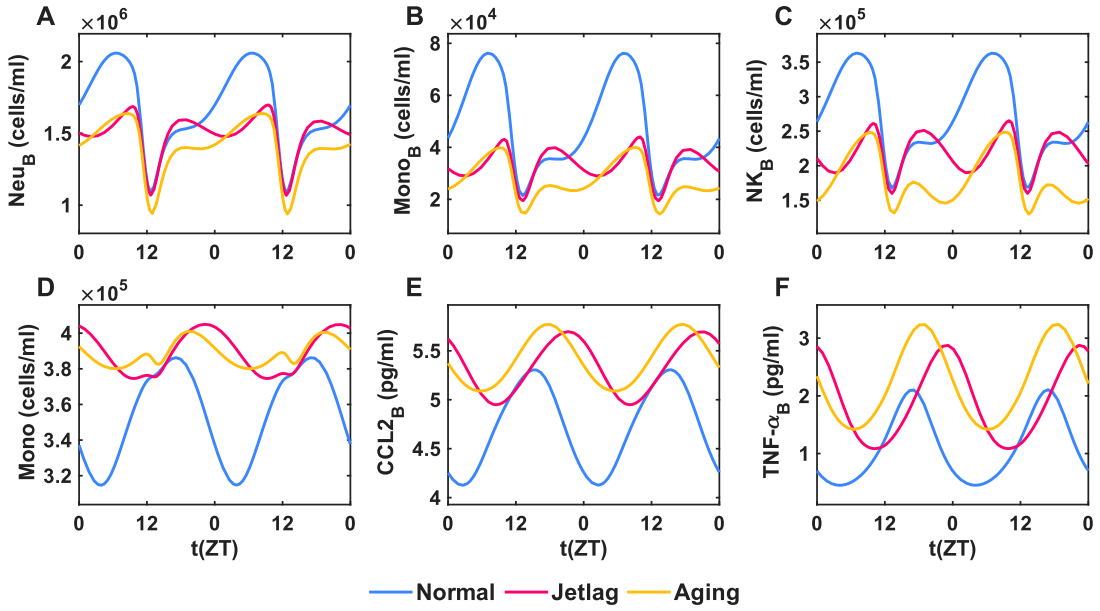

Figure 4. Simulated diurnal oscillations of immune-cell abundance and inflammatory cytokines regulated by circadian clocks that are disrupted by jet lag or aging under homeostasis, in comparison with those under the control of normal circadian clocks. Circadian rhythms are demonstrated for (A) neutrophils in blood ($\mathrm{Neu_B}$), (B) monocytes in blood ($\mathrm{Mono_B}$), (C) NK cells in blood ($\mathrm{NK_B}$), (D) monocytes in tissue (Mono), (E) CCL2 in blood ($\mathrm{CCL2_B}$), and (F) TNF-α in blood ($\mathrm{TNFa_B}$). Blue, magenta, and yellow lines denote the normal, jet-lagged, and aging conditions, respectively.

3.2. Exaggerated Acute Inflammatory Responses Under the Regulation of jet-Lagged And Aged Circadian Clocks

We next simulated the dynamic innate immune response in mice challenged with lipopolysaccharide (LPS), with the results presented in Figure 5. Under the same LPS dosage (3 mg/kg), the magnitude of the innate immune response was found to be dependent on the circadian clock. As shown in Figure 5A, under dysregulated circadian control induced by aging [33], the response of TNF-α, a core inflammatory cytokine in the innate immune system, was significantly stronger than that under normal circadian regulation with higher peak concentrations and prolonged inflammation compared to normal controls, indicating that aged individuals mount a more severe

 doi:10.20944/preprints202606.0096.v1

inflammatory response to pathogens. Similarly, Figure 5B illustrates the dynamic response of IL-10, a typical anti-inflammatory cytokine, upon pathogenic stimulation, and shows that its response amplitude in aged mice is also markedly higher than in young mice. The simulation results of Figures 5A and 5B agree well the experimental measurements. In mice subjected to jet lag [30], experimental challenge with lipopolysaccharide (LPS) also elicited a stronger innate immune response than that observed in control mice under normal conditions. We also simulated the innate immune response under dysregulated circadian control induced by jet lag. Figure 5C–E show the blood concentrations of the inflammatory cytokine TNF-α, the pro-inflammatory cytokine interleukin-1β (IL-1β), and the anti-inflammatory cytokine IL-10, simulated at 1.5 hours after LPS challenge (12.5 mg/kg), in comparison with experimental measurements [30]. The results demonstrate that the same dose of endotoxin provokes a stronger innate inflammatory response in both aged and jet-lagged mice than in normal mice, which are in general agreement with the experimental findings.

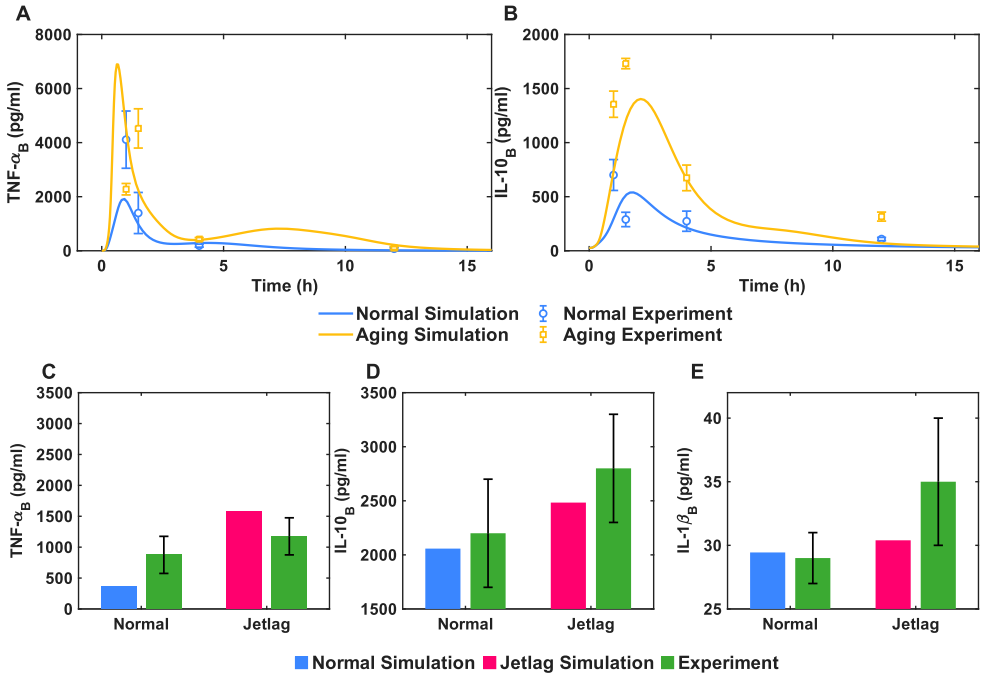

Figure 5. Simulated cytokine responses to LPS stimulation under normal, aged, and jet-lagged circadian conditions compared with experimental data. (A, B) Time courses of innate-immune cytokines in blood after LPS stimulation (3 mg/kg) at ZT21, regulated by normal (blue) and aged (yellow) clocks: (A) TNF-α and (B) IL-10. Lines represent simulation results, and symbols denote experimental data [33]. (C–E) Comparison of acute cytokine responses in blood 1.5 h after LPS stimulation (12.5 mg/kg) at ZT3 between the normal and jet-lagged clocks: (C) TNF-α, (D) IL-10, and (E) IL-1β. Blue bars indicate simulation results for the normal model, magenta bars indicate simulation results for the jet-lagged model, and green bars represent experimental data [30].

A 6. A–D. Under the same dose of LPS stimulation (3 mg/kg), the dynamic responses of cytokines TNF-α, IL-10, IL-1β, and CCL2 within 10 hours after LPS stimulation were strongest under the regulation of the aged circadian clock, followed by those under the jet-lagged circadian clock. Inflammatory cytokine responses under both conditions exhibited greater intensity and longer duration than those under normal circadian control, with particularly pronounced differences in peak levels. Figures 6E and 6F show neutrophil and CXCL5 dynamics over an extended 500-hour time course after LPS stimulation, further demonstrating that the innate immune response under disrupted circadian clock regulation exhibits a stronger inflammatory response compared to normal conditions and incurs a chronic low-grade inflammation [61].

 doi:10.20944/preprints202606.0096.v1

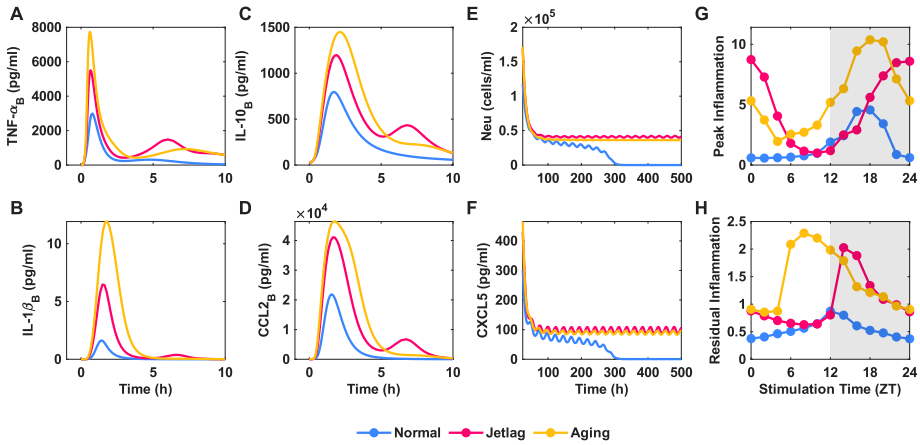

Figure 6. Exaggerated inflammatory responses under the regulation of jet-lagged and aged circadian clocks following LPS stimulation (3 mg/kg). (A-D) Acute cytokine response curves within 10 h post LPS stimulation at ZT20: (A) TNF-α, (B) IL-10, (C) IL-1β, and (D) CCL2. Disrupted circadian rhythms (jet-lagged and aged circadian clock) exhibit markedly higher peak cytokine levels relative to the normal circadian rhythm (blue). (E–F) Long-term resolution dynamics of neutrophil counts (Neu) and CXCL5 concentrations over 500 h post-stimulation. (G–H) The peak and residual inflammation coefficients, defined in Eqs. (1) and (2), are plotted as functions of LPS stimulation time, revealing that disrupted circadian regulation exhibits persistent elevation indicative of chronic inflammation.

Figure 6A–F showed the results of LPS stimulation at a specific time of day (ZT20). To delineate inflammatory responses for LPS applied at different time across the day and comprehensively compare inflammatory intensity under normal and disrupted circadian regulation, we systematically simulated innate immune responses in mice receiving an identical LPS dose (3 mg/kg) *at 12 day time points (i.e.,* t_i, *i=1, 2,…,12 for ZT2, ZT4, …,ZT24).* For the LPS challenge at time t_i, we determined from the simulated innate immune response the peak cytokine concentration $P_{j,k}(t_i)$, where *j* denotes one of the cytokines (TNF-α, IL-10, IL-1β, CCL2, or CXCL5), and *k* corresponds to the normal, jet-lagged, or aged circadian clock regulation. Similarly, the residual inflammation can be quantified by the cytokine level $R_{j,k}(t_i)$ at 12 hours after LPS challenge at time t_i. In terms of $P_{j,k}(t_i)$ *and* $R_{j,k}(t_i)$, a peak inflammation coefficient (PIC) and a residual inflammation coefficient (RIC) can be defined to **quantitatively evaluate the magnitude and persistence of inflammatory responses, both of which depend on the LPS stimulation time** t_i **and the normality or dysregulation of circadian rhythms (subscript-k-dependent),**

$$PIC_k(t_i) = \sum_j \frac{P_{j,k}(t_i)}{\text{Max}\{P_{j,k}(t_i),\ i=1,2,\ldots12,\ k=\text{normal}\}}, \quad (1)$$

$$RIC_k(t_i) = \sum_j \frac{R_{j,k}(t_i)}{\text{Max}\{R_{j,k}(t_i),\ i=1,2,\ldots12,\ k=\text{normal}\}}, \quad (2)$$

where the coefficients are normalized respectively to the maximum values of $P_{j,k}(t_i)$ *and* $R_{j,k}(t_i)$ simulated under **normal circadian regulation**. Figure 6G–H depicts PIC and RIC as functions of LPS stimulation time. The results reveal that the magnitude and persistence of acute inflammatory burden under regulation of jet-lagged and aged circadian clocks are systematically higher than those under normal circadian regulation. Together, the increased residual inflammatory score and the persistent CXCL5 elevation are consistent with reduced inflammation resolution and the emergence of chronic low-grade inflammation [61].

 doi:10.20944/preprints202606.0096.v1

3.3.. Mechanism of Exaggerated Acute Inflammation Induced by Circadian Disruption

The mechanism of exaggerated inflammation induced by jet-lagged and aged circadian clocks is rooted in the inflammatory response that is regulated by core clock proteins such as BMAL1–CLOCK, RORs, and CORT. In innate immunity, inflammatory responses involving cytokines TNF-α, IL-β, IL-10, and etc. is tightly related with the monocyte–TNF-α positive feedback loop. Upon activation, monocytes rapidly secrete the pro-inflammatory cytokines TNF-α and IL-1β. TNF-α facilitates monocyte recruitment from the circulation into peripheral tissues and further promotes their tissue-level activation, whereas IL-1β released by activated monocytes in turn augments TNF-α production, thereby forming a self-amplifying positive feedback loop of inflammation. The feedback circuit is under circadian regulation via clock proteins: the CLOCK–BMAL1 complex suppresses TNF-α synthesis, ROR family proteins constrain TNF-α production, and the immunosuppressive hormone CORT also downregulates TNF-α secretion. To explore the dynamic mechanism, we extracted the ODEs governing monocytes and TNF-α for separate analysis, which are presented in the following form (see Supplementary Eqs. S16 and S27),

$$\frac{d[\mathrm{Mono}]}{dt} = -d_{\mathrm{Mono}} \cdot [\mathrm{Mono}] + B_{\mathrm{Mono}} \left(1 + \frac{h_{\mathrm{TNFa\_Mono}} \cdot [\mathrm{TNFa}]^3}{K^3_{\mathrm{TNFa\_Mono}} + [\mathrm{TNFa}]^3}\right), \quad (3)$$

$$\frac{d[\mathrm{TNFa}]}{dt} = -d'_{\mathrm{TNFa}} \cdot [\mathrm{TNFa}] + C_{\mathrm{TNFa}} \cdot \frac{([\mathrm{Mono}] \cdot AR)^4}{([\mathrm{Mono}] \cdot AR)^4 + K^4_{\mathrm{TNFa_{Mono}}}}, \quad (4)$$

where d'_{TNFa} is the effective decay rate which has merged the decay of TNF-α and its diffusions into the circulation. Equations 3 and 4 are non-autonomous which depend on the dynamic variable *AR* (i.e., the fraction of activated monocytes in tissue) and time dependent parameters B_{Mono} and C_{TNFa} defined by,

$$B_{\mathrm{Mono}} \equiv c_{\mathrm{CCL2\_Mono}} \cdot \frac{[\mathrm{MonoBlood}]^2}{[\mathrm{MonoBlood}]^2 + K^2_{\mathrm{BT\_Mono}}} \cdot \frac{[\mathrm{CCL2}]^4}{K^4_{\mathrm{CCL2\_Mono}} + [\mathrm{CCL2}]^4}, \quad (5)$$

$$C_{TNFa} \equiv c_{\mathrm{Mono\_TNFa}} \cdot \frac{K^3_{\mathrm{IL10\_TNFa}}}{K^3_{\mathrm{IL10\_TNFa}} + [\mathrm{IL10}]^3} \cdot \left(1 + h_{\mathrm{IL1b\_TNFa}} \cdot \frac{[\mathrm{IL1b}]^3}{K^3_{\mathrm{IL1b\_TNFa}} + [\mathrm{IL1b}]^3}\right) \cdot \frac{K^4_{\mathrm{ROR\_TNFa}}}{K^4_{\mathrm{ROR\_TNFa}} + [\mathrm{ROR}]^4} \cdot \frac{K^3_{\mathrm{BC_{TNFa}}}}{K^3_{\mathrm{BC\_TNFa}} + [\mathrm{BMAL1-CLOCK}]^3} \cdot \frac{K^2_{\mathrm{CORT\_TNFa}}}{K^2_{\mathrm{CORT\_TNFa}} + [\mathrm{CORT}]^2}. \quad (6)$$

B_{Mono} and C_{TNFa} represent the recruitment rate of monocytes from the bloodstream and the secretion rate of TNF-α, respectively. Simulations indicate that B_{Mono} varies little over time and is unaffected by the circadian clock. In the subsequent analysis, B_{Mono} is set as a fixed parameter, whereas *AR* and C_{TNFa} serve as control parameters. In Equation 6, C_{TNFa} is dynamically regulated by the circadian clock through BMAL1-CLOCK, RORs, and CORT. Figure 7A depicts the bifurcation diagram for Equations (3) and (4), illustrating how the steady state varies with AR and C_{TNFa} and revealing a folded bistable surface. Figure 7A also shows the trajectories of (AR, C_{TNFa}, TNF-α) under regulation of normal, jet-lagged, and aged circadian rhythms. Figure 7B presents the projections of steady-state surface in Figure 7A together with the three trajectories onto the $AR - C_{\mathrm{TNFa}}$ parameter plane. The two trajectories corresponding to aberrant circadian rhythms cross the bistable regime and invade into the high TNF-α state which corresponds to the high inflammation state. Figures 7C and 7D display cross-sections of the steady-state surface in Figure 7 at fixed values of C_{TNFa} and *AR*, clearly illustrating the saddle-node bifurcation in Equations (3) and (4). Figure 7E,F show the time courses of C_{TNFa} and *AR*, which act as control parameters in the two-variable dynamical system of Equations (3) and (4). Notably, C_{TNFa} exhibits strong dependence on circadian

 doi:10.20944/preprints202606.0096.v1

rhythm, with its variation range differing markedly between normal and the two aberrant circadian conditions. *AR* exhibits negligible dependence on circadian clock types but undergoes activation and subsequent decline upon LPS stimulation. In Figure 7E, C_{TNFa} ranges from 1×10^7 to 4×10^7, remaining confined to the low-inflammatory state in the bistable regime and failing to cross the right-side saddle-node point in Figure 7C to access the hyperinflammatory state. In contrast, under jet-lagged and aged circadian clock regulation, C_{TNFa} exceeds this saddle-node point, enabling the system to dynamically transition into the hyperinflammatory state. This observation is consistent with the trajectory shown in Figure 7B.

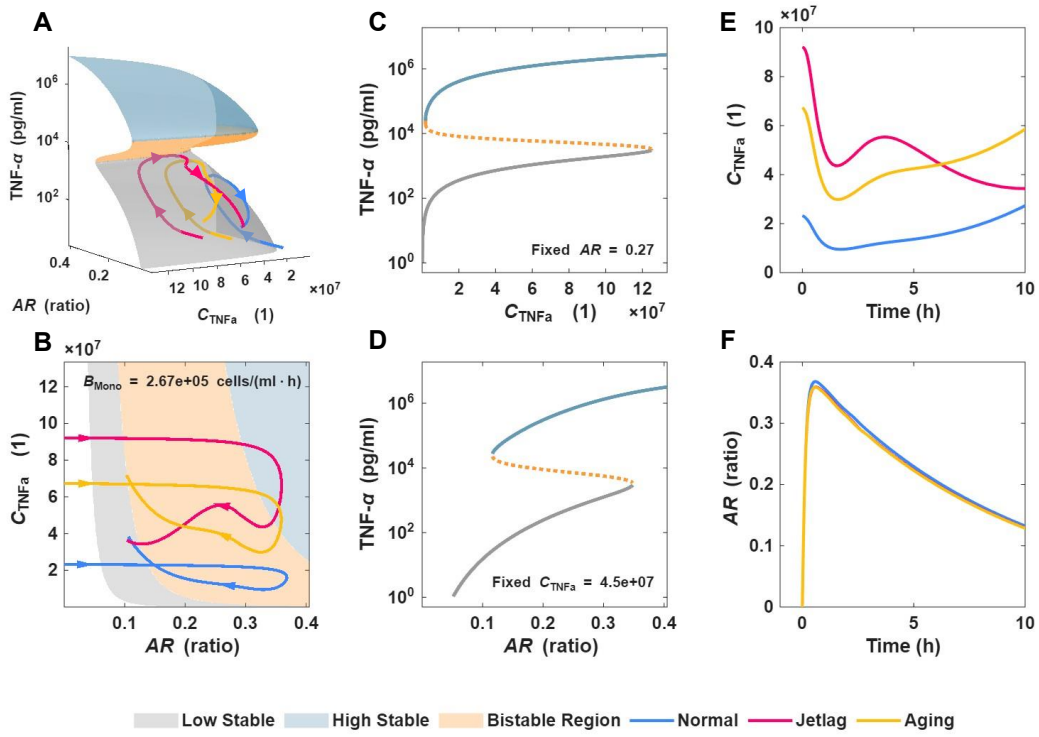

Figure 7. Bifurcation analysis of the two-variable system described by Equations 3 and 4, with *AR* and C_{TNFa} taken as control parameters. (A) Steady-state surface as a function of *AR* and C_{TNFa}, along with the trajectories of (AR, C_{TNFa}, TNF-α) under normal, jet-lagged, and aged circadian rhythms. (B) Projections of the steady-state surface and the three trajectories in panel (A) onto the *AR*-C_{TNFa} plane, showing monostable and bistable regions as well as the trajectory evolution across these regimes. (C,D) Two-dimensional cross-sections of the bifurcation surface at fixed *AR*=0.27 (C) and fixed $C_{\mathrm{TNF}\alpha} = 4.5 \times 10^7$ (D), illustrating saddle-node bifurcations and bistability characteristics. (E,F) Time courses of C_{TNFa} (E) and *AR* (F) under normal, jet-lagged, and aged circadian rhythms. The trajectories are generated with a LPS dose of 2 mg/kg administered at ZT0.

The mechanism of enhanced inflammation induced by circadian disruption shown in Figure 7 can be further elucidated by the trajectories on monocyte–TNF-α phase plane in Figure 8. The transient trajectories under the regulation of normal and two aberrant circadian clocks are simulated with an endotoxin challenge (3 mg/kg LPS). In Figure 8, the "S"-shaped monocyte nullcline (d[Mono]/dt = 0) remains fixed, whereas the nearly straight TNF-α nullcline (d[TNFa]/dt = 0) shifts upper-left with variations in *AR* and $\boldsymbol{C_{\mathrm{TNFa}}}$. During this process, the number of intersection points between the two nullclines transiently changes from one to two and eventually returns to one via saddle-node bifurcation. Initially, the intersection of the two nullclines gives rise to a single high steady-state fixed point (high-inflammation), which attracts system trajectories toward itself eliciting an acute inflammatory response. As the TNF-α nullcline shifts, a low steady-state fixed point gradually emerges to ensure a self-limiting inflammatory response, while the high steady-state fixed

 doi:10.20944/preprints202606.0096.v1

point is annihilated thereafter. Correspondingly, the system trajectory rises to a peak and then declines, eventually being attracted and settling into the low monostable steady state (low-inflammation). Under normal circadian clock regulation (Figure 8A–D), the trajectory remains confined within the low-inflammatory region. By contrast, under jet-lagged (Figure 8E–H) and aged (Figure 8I–L) circadian clock regulation, the trajectory departs substantially from the low-inflammatory region, crosses the saddle point between the two bistable states transiently, and moves toward the high-state fixed point. Although the trajectory eventually converges to the low-state fixed point in all three cases, it sustains a prolonged residence within the hyperinflammatory region under aberrant circadian conditions. These analyses uncover a dynamic mechanism underlying how disrupted circadian clocks drive exaggerated acute inflammatory responses.

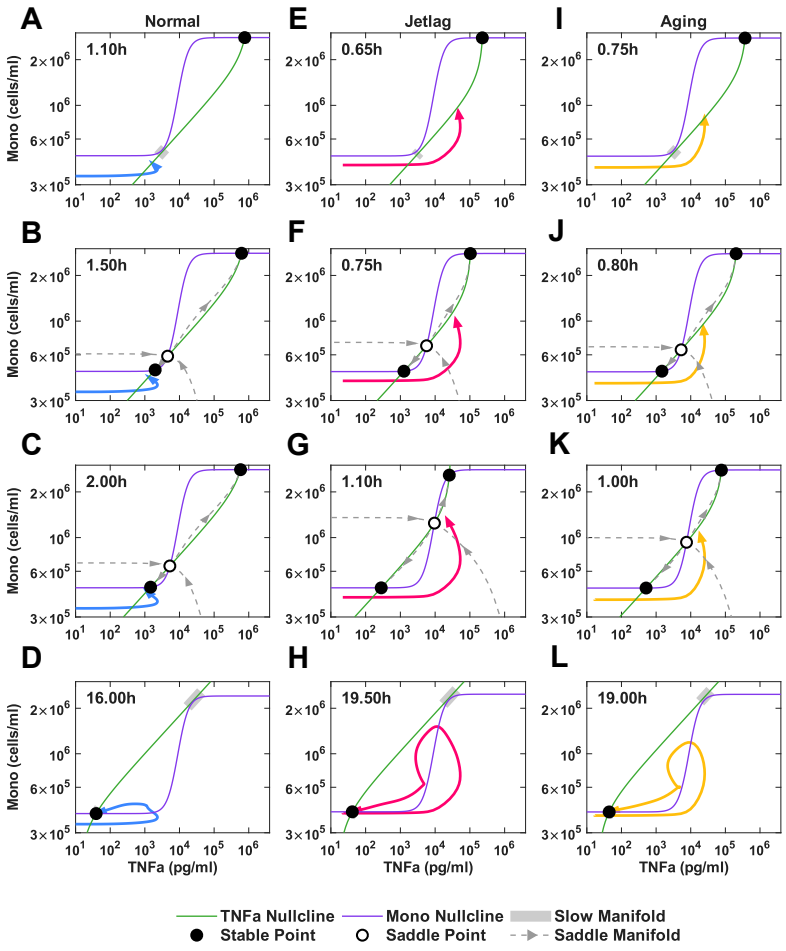

Figure 8. Time-resolved snapshots of trajectories in the monocyte–TNF-α phase plane following LPS stimulation (3 mg/kg) at ZT0. Columns show trajectories under normal (A–D), jet-lagged (E–H), and aged (I–L) circadian clock regulations. The system exhibits a prolonged residence in the hyperinflammatory region under jet-lagged and aged circadian clock conditions.

Long after antigen challenge, most variables in the system decline to very low levels, while a small number remain at relatively high magnitudes. Long-time persistent higher level in neutrophil and CXCL5 shown in Figures 6E-F suggests a chronic low-grade inflammation that disrupted circadian clocks incur. As we have checked, the dynamic origin for the emergence of chronic low-grade inflammation lies in the positive feedback loop in which neutrophils secret the chemokine CXCL5 that enhances its migration from blood to tissue. The positive feedback loop is regulated by the circadian clock in which the production of CXCL5 is repressed by BMAL1–CLOCK. Saddle-node

 doi:10.20944/preprints202606.0096.v1

bifurcation and bistability occurs in the two-variable neutrophils-CXCL5 ODEs (see Supplementary Equations S35 and S36) as illustrated in Figure 9. It depicts that the fluctuation range under a normal circadian clock spans both the "single low state" region and the "bistability" region, enabling the system to gradually return to the low state after stimulation, whereas the fluctuation ranges under disrupted circadian clocks cover mainly the "bistability" region, so once the system is activated into the high state, it ultimately stabilizes in the high-inflammation state. This explains why circadian disruption can induce chronic inflammation.

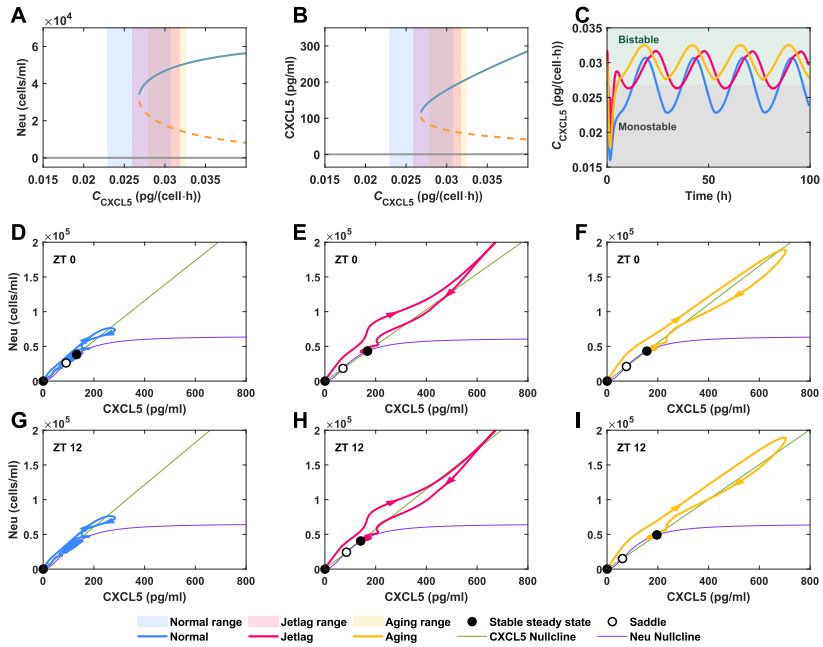

Figure 9. Neutrophil-CXCL5 positive feedback-mediated bistability (A-C) and circadian clock-regulated dynamics under normal (D,G), jet-lagged (E, H) and aged (F, I) conditions after prolonged antigen stimulation. The trajectories in panels D–I represent simulation results of LPS stimulation at a dose of 2.25 mg/kg: panels D–F correspond to ZT0 stimulation, and panels G–I to ZT12 stimulation. The bifurcation diagrams (A,B) are obtained on the base of the isolated 2-varaible ODEs for neutrophil and CXCL5 (see Supplementary Equations S35 and S36), where C_{CXCL5} is the control parameter influenced by the circadian clock.

4. Discussion

The circadian clock significantly influences innate immune processes, and its disruption impairs immune responses. Immune dysregulation can trigger acute cytokine storms and chronic inflammation (e.g., inflammaging), which can culminate in immune-mediated inflammatory diseases (IMIDs), including autoimmune disorders. While these effects are well-documented experimentally, the underlying quantitative dynamic mechanisms remain incompletely understood. Here we proposed a comprehensive model that integrates currently known interactions through which the circadian clock modulates innate immunity. This model encompasses the regulatory roles of both the canonical TTFL circadian machinery and rhythmic CORT signaling within the HPA axis. We further explore the dynamic mechanisms by which circadian disruption drives exaggerated inflammatory responses: the circadian clock modulates bistability arising from pro-inflammatory feedback loops, thereby governing residence times in low- and high-inflammation states, and shaping the magnitude and duration of inflammatory responses. With properly calibrated parameters, the model recapitulates homeostatic circadian oscillations and exaggerated acute inflammatory responses to antigen challenge under normal, jet-lagged, and aging circadian conditions, consistent with experimental observations. This framework provides a mechanistic dynamic interpretation of how

 doi:10.20944/preprints202606.0096.v1

circadian disruption exacerbates acute inflammatory injury and drives chronic inflammation, filling a critical knowledge gap in prior qualitative studies.

The uncovered mechanism sheds light on immune dysregulation linked to diverse circadian rhythm disorders and underscores the therapeutic potential of circadian-targeted strategies. Multiple clock-targeted interventions have been reported to ameliorate immune dysregulation [62]. For example, melatonin—a key circadian hormone—can reduce neutrophil infiltration and the release of pro-inflammatory cytokines during acute inflammation, thereby limiting tissue injury [63]. In mice, REV-ERBα agonists strengthen circadian oscillations and attenuate adaptive-immune overactivation, reducing disease severity in experimental autoimmune encephalomyelitis (EAE) and inflammatory bowel diseases (IBD) [64]. More recently, the plant-derived compound jujuboside A (JuA) has been shown to modulate (e.g., inhibit) NF-κB signaling, thereby enhancing clock-linked anti-inflammatory effects and reducing dysregulated production of inflammatory cytokines [65]. Guided by our model's insights, we suggest that these interventions may confer therapeutic benefits by: (1) restoring robust, physiological-amplitude circadian oscillations within innate immune pathways; (2) enhancing system robustness to perturbations (i.e., enlarge the basin of attraction of the low-inflammation state); and (3) raising the switching threshold, thereby reducing transitions to the high-inflammation state. In the future, by combining this model with disease-specific characteristics, one can design targeted chronotherapies to prevent and treat damage caused by excessive immune responses. Finally, our framework provides a scalable foundation for exploring the circadian regulation of adaptive immunity and behavior.

Several limitations of this study should be noted. First, our model adopts a framework of unidirectional regulation (from the clock to immunity), but in recent years several experiments have reported feedback effects of inflammation on the clock that lead to circadian disruption [66]. For example, the NF-κB pathway, which is activated at the same time of inflammation, upregulates miR-155. This microRNA directly targets and degrades *Bmal1* mRNA, disturbing the core clock loop [67]. Meanwhile, pro-inflammatory cytokines can also affect the clock: TNF-α can inhibit the expression of clock genes by interfering with E-box-mediated transcription [68]; IL-1β can enhance the degradation efficiency of REV-ERB protein via the ubiquitin–proteasome pathway, thereby suppressing its concentration [69]. Some models have already taken related aspects into account by adding pathways through which inflammatory cytokines feed back onto clock proteins [39,70]. Furthermore, as our current framework focuses on the acute-phase kinetics of inflammation, it does not explicitly model tissue injury or the subsequent liberation of damage-associated molecular patterns (DAMPs). These secondary processes often trigger more severe cytokine storms and typically manifest on a timescale extending beyond the immediate acute response modeled here. In this context, the exaggerated short-term inflammatory bursts predicted by our model serve as a precursor indicator for such pathological risks; an intensified acute response implies a higher probability of crossing the threshold into uncontrolled systemic damage [71]. Future models need to incorporate feedback loops and DAMPs to more realistically simulate the progression of chronic inflammation. Our model focuses only on two types of circadian disruption—jet lag and aging—whereas in practice different rhythm disorders (e.g., repeated phase shifts in shift work, circadian desynchrony among organs [30]) may have differential effects on immunity. Future work could construct more fine-grained models of circadian disruptions and introduce quantitative metrics that jointly assess host-protection efficacy and immunopathology, enabling comparison of immune outcomes across different forms of circadian disruption. This may also help reveal how the immune system has evolved trade-offs between costs and benefits during evolution to ultimately form its current complex architecture—strong and powerful enough for defense, yet without incurring excessive immune damage too frequently [72,73]. Furthermore, our representation of neuroendocrine regulation remains simplified. By modeling CORT dynamics solely through empirical functions, we treated the HPA axis as the exclusive regulatory pathway, neglecting the critical role of the sympathetic nervous system (SNS). Crucially, catecholamines regulate leukocyte trafficking via mechanisms distinct from glucocorticoids. For instance, catecholamines trigger rapid mobilization of

 doi:10.20944/preprints202606.0096.v1

leukocytes from the marginal pool during acute stress [74]. Consequently, the absence of adrenergic variables prevents our model from capturing the dynamics of early immune mobilization. Future comprehensive models should integrate these signaling pathways to fully reflect stress physiology.

5. Conclusions

We developed a mechanistic, multi-compartment mathematic model linking innate immunity to distinct circadian clocks (normal or disturbed). The model quantitatively reproduces daily rhythms in leukocyte trafficking and cytokine secretion, as well as acute immune responses to endotoxin challenge under the regulation of the normal and disruption clock induced by jet lag or aging. The results indicate that the framework captures key features of circadian gating of innate immune responses at both molecular and systems levels. The model provides a compact dynamics view of how clock disruption can shift innate immunity toward more persistent and exaggerated inflammatory responses. Instead of merely scaling cytokine levels, circadian disruption alters core inflammatory circuits, making the system more prone to high and sustained activation following transient stimuli. This perspective offers a unifying explanation for a wide range of experimental and clinical observations linking disturbed circadian rhythms to dysregulated inflammation. More broadly, our framework provides a quantitative foundation for virtual chronotherapy simulations. By systematically modulating circadian perturbations or integrating disease- and tissue-specific modules into the current model, future work could explore how clock-targeted or time-of-day-based interventions prevent and mitigate immune-mediated tissue damage. Ultimately, our findings highlight that sustaining robust circadian rhythms constitutes a fundamental strategy to keep innate immune responses protective yet self-limiting, thereby maintaining systemic physiological homeostasis.

Supplementary Materials: The following supporting information can be downloaded at the website of this paper posted on Preprints.org.

Author Contributions: Q.Z. performed the simulations and analyzed the results. H.W and Q.O. conceived the project. Q.Z. and H.W. wrote the paper. All authors reviewed the manuscript.

Funding: This work was supported by the National Natural Science Foundation of China (12090051 to HW), and the Starry Night Science Fund of Zhejiang University Shanghai Institute for Advanced Study (to QO). The funders had no role in study design, data collection and analysis, decision to publish, or preparation of the manuscript.

Conflicts of Interest: The authors declare no competing interests.

References

1. Druzd, D.; de Juan, A.; Scheiermann, C. Circadian Rhythms in Leukocyte Trafficking. *Semin Immunopathol* **2014**, *36*, 149–162, doi:10.1007/s00281-013-0414-4.
2. Man, K.; Loudon, A.; Chawla, A. Immunity around the Clock. *Science* **2016**, *354*, 999–1003, doi:10.1126/science.aah4966.
3. Li, W.; Wang, Z.; Cao, J.; Dong, Y.; Chen, Y. Perfecting the Life Clock: The Journey from PTO to TTFL. *Int J Mol Sci* **2023**, *24*, 2402, doi:10.3390/ijms24032402.
4. Rabinovich-Nikitin, I.; Kirshenbaum, E.; Kirshenbaum, L.A. Autophagy, Clock Genes, and Cardiovascular Disease. *Can J Cardiol* **2023**, *39*, 1772–1780, doi:10.1016/j.cjca.2023.08.022.
5. Chong, S.Z.; Evrard, M.; Devi, S.; Chen, J.; Lim, J.Y.; See, P.; Zhang, Y.; Adrover, J.M.; Lee, B.; Tan, L.; et al. CXCR4 Identifies Transitional Bone Marrow Premonocytes That Replenish the Mature Monocyte Pool for Peripheral Responses. *J Exp Med* **2016**, *213*, 2293–2314, doi:10.1084/jem.20160800.
6. Lucas, D.; Battista, M.; Shi, P.A.; Isola, L.; Frenette, P.S. Mobilized Hematopoietic Stem Cell Yield Depends on Species-Specific Circadian Timing. *Cell Stem Cell* **2008**, *3*, 364–366, doi:10.1016/j.stem.2008.09.004.

 doi:10.20944/preprints202606.0096.v1

7. Méndez-Ferrer, S.; Lucas, D.; Battista, M.; Frenette, P.S. Haematopoietic Stem Cell Release Is Regulated by Circadian Oscillations. *Nature* **2008**, *452*, 442–447, doi:10.1038/nature06685.
8. He, W.; Holtkamp, S.; Hergenhan, S.M.; Kraus, K.; De Juan, A.; Weber, J.; Bradfield, P.; Grenier, J.M.P.; Pelletier, J.; Druzd, D.; et al. Circadian Expression of Migratory Factors Establishes Lineage-Specific Signatures That Guide the Homing of Leukocyte Subsets to Tissues. *Immunity* **2018**, *49*, 1175-1190.e7, doi:10.1016/j.immuni.2018.10.007.
9. Hayashi, M.; Shimba, S.; Tezuka, M. Characterization of the Molecular Clock in Mouse Peritoneal Macrophages. *Biol Pharm Bull* **2007**, *30*, 621–626, doi:10.1248/bpb.30.621.
10. Kitchen, G.B.; Cunningham, P.S.; Poolman, T.M.; Iqbal, M.; Maidstone, R.; Baxter, M.; Bagnall, J.; Begley, N.; Saer, B.; Hussell, T.; et al. The Clock Gene Bmal1 Inhibits Macrophage Motility, Phagocytosis, and Impairs Defense against Pneumonia. *Proc. Natl. Acad. Sci. U.S.A.* **2020**, *117*, 1543–1551, doi:10.1073/pnas.1915932117.
11. Keller, M.; Mazuch, J.; Abraham, U.; Eom, G.D.; Herzog, E.D.; Volk, H.-D.; Kramer, A.; Maier, B. A Circadian Clock in Macrophages Controls Inflammatory Immune Responses. *Proc. Natl. Acad. Sci. U.S.A.* **2009**, *106*, 21407–21412, doi:10.1073/pnas.0906361106.
12. Nguyen, K.D.; Fentress, S.J.; Qiu, Y.; Yun, K.; Cox, J.S.; Chawla, A. Circadian Gene Bmal1 Regulates Diurnal Oscillations of Ly6Chi Inflammatory Monocytes. *Science* **2013**, *341*, 1483–1488, doi:10.1126/science.1240636.
13. Silver, A.C.; Arjona, A.; Walker, W.E.; Fikrig, E. The Circadian Clock Controls Toll-like Receptor 9-Mediated Innate and Adaptive Immunity. *Immunity* **2012**, *36*, 251–261, doi:10.1016/j.immuni.2011.12.017.
14. Griffin, P.; Sheehan, P.W.; Dimitry, J.M.; Guo, C.; Kanan, M.F.; Lee, J.; Zhang, J.; Musiek, E.S. REV-ERBα Mediates Complement Expression and Diurnal Regulation of Microglial Synaptic Phagocytosis. *eLife* **2020**, *9*, e58765, doi:10.7554/eLife.58765.
15. Lang, V.; Ferencik, S.; Ananthasubramaniam, B.; Kramer, A.; Maier, B. Susceptibility Rhythm to Bacterial Endotoxin in Myeloid Clock-Knockout Mice. *eLife* **2021**, *10*, e62469, doi:10.7554/eLife.62469.
16. Desmet, L.; Thijs, T.; Mas, R.; Verbeke, K.; Depoortere, I. Time-Restricted Feeding in Mice Prevents the Disruption of the Peripheral Circadian Clocks and Its Metabolic Impact during Chronic Jetlag. *Nutrients* **2021**, *13*, 3846, doi:10.3390/nu13113846.
17. Gibbs, J.; Ince, L.; Matthews, L.; Mei, J.; Bell, T.; Yang, N.; Saer, B.; Begley, N.; Poolman, T.; Pariollaud, M.; et al. An Epithelial Circadian Clock Controls Pulmonary Inflammation and Glucocorticoid Action. *Nat Med* **2014**, *20*, 919–926, doi:10.1038/nm.3599.
18. Liu, J.; Mustafa, S.; Barratt, D.T.; Hutchinson, M.R. Corticosterone Preexposure Increases NF-κB Translocation and Sensitizes IL-1β Responses in BV2 Microglia-Like Cells. *Front. Immunol.* **2018**, *9*, 3, doi:10.3389/fimmu.2018.00003.
19. Lim, H.-Y.; Müller, N.; Herold, M.J.; van den Brandt, J.; Reichardt, H.M. Glucocorticoids Exert Opposing Effects on Macrophage Function Dependent on Their Concentration. *Immunology* **2007**, *122*, 47–53, doi:10.1111/j.1365-2567.2007.02611.x.
20. Hwang, J.-W.; Sundar, I.K.; Yao, H.; Sellix, M.T.; Rahman, I. Circadian Clock Function Is Disrupted by Environmental Tobacco/Cigarette Smoke, Leading to Lung Inflammation and Injury via a SIRT1-BMAL1 Pathway. *FASEB J* **2014**, *28*, 176–194, doi:10.1096/fj.13-232629.
21. Xiong, X.-Y.; Liang, J.; Xu, Y.-Q.; Liu, Y. The Tilapia Collagen Peptide Mixture TY001 Protects against LPS-Induced Inflammation, Disruption of Glucose Metabolism, and Aberrant Expression of Circadian Clock Genes in Mice. *Chronobiol Int* **2019**, *36*, 1013–1023, doi:10.1080/07420528.2019.1606821.
22. Huang, S.; Jiao, X.; Lu, D.; Pei, X.; Qi, D.; Li, Z. Light Cycle Phase Advance as a Model for Jet Lag Reprograms the Circadian Rhythms of Murine Extraorbital Lacrimal Glands. *Ocul Surf* **2021**, *20*, 95–114, doi:10.1016/j.jtos.2021.02.001.
23. Kumar, A.; Vaca-Dempere, M.; Mortimer, T.; Deryagin, O.; Smith, J.G.; Petrus, P.; Koronowski, K.B.; Greco, C.M.; Segalés, J.; Andrés, E.; et al. Brain-Muscle Communication Prevents Muscle Aging by Maintaining Daily Physiology. *Science* **2024**, *384*, 563–572, doi:10.1126/science.adj8533.
24. Chen, Y.-C.; Wang, W.-S.; Lewis, S.J.G.; Wu, S.-L. Fighting Against the Clock: Circadian Disruption and Parkinson's Disease. *J Mov Disord* **2024**, *17*, 1–14, doi:10.14802/jmd.23216.

 doi:10.20944/preprints202606.0096.v1

25. Chen, R.; Weitzner, A.S.; McKennon, L.A.; Fonken, L.K. Light at Night during Development in Mice Has Modest Effects on Adulthood Behavior and Neuroimmune Activation. *Behav Brain Res* **2021**, *405*, 113171, doi:10.1016/j.bbr.2021.113171.
26. Laxmi, I.P.L.; Tamizhselvi, R. Epigenetic Events Influencing the Biological Clock: Panacea for Neurodegeneration. *Heliyon* **2024**, *10*, e38836, doi:10.1016/j.heliyon.2024.e38836.
27. Xie, M.; Tang, Q.; Nie, J.; Zhang, C.; Zhou, X.; Yu, S.; Sun, J.; Cheng, X.; Dong, N.; Hu, Y.; et al. BMAL1-Downregulation Aggravates Porphyromonas Gingivalis-Induced Atherosclerosis by Encouraging Oxidative Stress. *Circ Res* **2020**, *126*, e15–e29, doi:10.1161/CIRCRESAHA.119.315502.
28. Scheiermann, C.; Kunisaki, Y.; Lucas, D.; Chow, A.; Jang, J.-E.; Zhang, D.; Hashimoto, D.; Merad, M.; Frenette, P.S. Adrenergic Nerves Govern Circadian Leukocyte Recruitment to Tissues. *Immunity* **2012**, *37*, 290–301, doi:10.1016/j.immuni.2012.05.021.
29. Mul Fedele, M.L.; Aiello, I.; Caldart, C.S.; Golombek, D.A.; Marpegan, L.; Paladino, N. Differential Thermoregulatory and Inflammatory Patterns in the Circadian Response to LPS-Induced Septic Shock. *Front. Cell. Infect. Microbiol.* **2020**, *10*, 100, doi:10.3389/fcimb.2020.00100.
30. Castanon-Cervantes, O.; Wu, M.; Ehlen, J.C.; Paul, K.; Gamble, K.L.; Johnson, R.L.; Besing, R.C.; Menaker, M.; Gewirtz, A.T.; Davidson, A.J. Disregulation of Inflammatory Responses by Chronic Circadian Disruption. *J. Immunol.* **2010**, *185*, 5796–5805, doi:10.4049/jimmunol.1001026.
31. Guerrero-Vargas, N.N.; Guzmán-Ruiz, M.; Fuentes, R.; García, J.; Salgado-Delgado, R.; Basualdo, M.D.C.; Escobar, C.; Markus, R.P.; Buijs, R.M. Shift Work in Rats Results in Increased Inflammatory Response after Lipopolysaccharide Administration: A Role for Food Consumption. *J Biol Rhythms* **2015**, *30*, 318–330, doi:10.1177/0748730415586482.
32. Jackson, D.M.; Castanon-Cervantes, O. Impaired Responses to In Vitro Lipopolysaccharide-Induced Stimulation After Long-Term, Rotating Shift Work. *Int J Environ Res Public Health* **2025**, *22*, 791, doi:10.3390/ijerph22050791.
33. Namas, R.A.; Bartels, J.; Hoffman, R.; Barclay, D.; Billiar, T.R.; Zamora, R.; Vodovotz, Y. Combined In Silico, In Vivo, and In Vitro Studies Shed Insights into the Acute Inflammatory Response in Middle-Aged Mice. *PLoS One* **2013**, *8*, e67419, doi:10.1371/journal.pone.0067419.
34. Youm, Y.-H.; Grant, R.W.; McCabe, L.R.; Albarado, D.C.; Nguyen, K.Y.; Ravussin, A.; Pistell, P.; Newman, S.; Carter, R.; Laque, A.; et al. Canonical Nlrp3 Inflammasome Links Systemic Low-Grade Inflammation to Functional Decline in Aging. *Cell Metab* **2013**, *18*, 519–532, doi:10.1016/j.cmet.2013.09.010.
35. Sang, D.; Lin, K.; Yang, Y.; Ran, G.; Li, B.; Chen, C.; Li, Q.; Ma, Y.; Lu, L.; Cui, X.-Y.; et al. Prolonged Sleep Deprivation Induces a Cytokine-Storm-like Syndrome in Mammals. *Cell* **2023**, *186*, 5500-5516.e21, doi:10.1016/j.cell.2023.10.025.
36. Roy, A.; Daun, S.; Clermont, G.; Rubin, J.; Vodovotz, Y.; Lagoa, C.; Parker, R. A Mathematical Model of Acute Inflammatory Response to Endotoxin Challenge. *AIChE Annual Meeting* **2007**, 538.
37. Daun, S.; Rubin, J.; Vodovotz, Y.; Roy, A.; Parker, R.; Clermont, G. An Ensemble of Models of the Acute Inflammatory Response to Bacterial Lipopolysaccharide in Rats: Results from Parameter Space Reduction. *J. Theor. Biol.* **2008**, *253*, 843–853, doi:10.1016/j.jtbi.2008.04.033.
38. Zhou, Z.; Li, D.; Zhao, Z.; Shi, S.; Wu, J.; Li, J.; Zhang, J.; Gui, K.; Zhang, Y.; Ouyang, Q.; et al. Dynamical Modelling of Viral Infection and Cooperative Immune Protection in COVID-19 Patients. *PLoS Comput Biol* **2023**, *19*, e1011383, doi:10.1371/journal.pcbi.1011383.
39. Abo, S.M.C.; Layton, A.T. Modeling the Circadian Regulation of the Immune System: Sexually Dimorphic Effects of Shift Work. *PLoS Comput Biol* **2021**, *17*, e1008514, doi:10.1371/journal.pcbi.1008514.
40. Balit, N.; Cermakian, N.; Khadra, A. The Influence of Circadian Rhythms on CD8+ T Cell Activation upon Vaccination: A Mathematical Modeling Perspective. *J. Theor. Biol.* **2024**, *590*, 111852, doi:10.1016/j.jtbi.2024.111852.
41. Weng, X.; Ouyang, Q.; Wang, H. Dynamic Mechanisms of Time-of-Day-Dependent Adaptive Immunity and Vaccination Responses. *Biophys. J.* **2026**, S0006349526000561, doi:10.1016/j.bpj.2026.01.041.
42. Wei, N.; Gumz, M.L.; Layton, A.T. Predicted Effect of Circadian Clock Modulation of NHE3 of a Proximal Tubule Cell on Sodium Transport. *Am J Physiol Renal Physiol* **2018**, *315*, F665–F676, doi:10.1152/ajprenal.00008.2018.

 doi:10.20944/preprints202606.0096.v1

43. Li, J.; Wu, J.; Zhang, J.; Tang, L.; Mei, H.; Hu, Y.; Li, F. A Multicompartment Mathematical Model Based on Host Immunity for Dissecting COVID-19 Heterogeneity. *Heliyon* **2022**, *8*, e09488, doi:10.1016/j.heliyon.2022.e09488.
44. Nagasawa, T.; Hirota, S.; Tachibana, K.; Takakura, N.; Nishikawa, S.; Kitamura, Y.; Yoshida, N.; Kikutani, H.; Kishimoto, T. Defects of B-Cell Lymphopoiesis and Bone-Marrow Myelopoiesis in Mice Lacking the CXC Chemokine PBSF/SDF-1. *Nature* **1996**, *382*, 635–638, doi:10.1038/382635a0.
45. Tachibana, K.; Hirota, S.; Iizasa, H.; Yoshida, H.; Kawabata, K.; Kataoka, Y.; Kitamura, Y.; Matsushima, K.; Yoshida, N.; Nishikawa, S.; et al. The Chemokine Receptor CXCR4 Is Essential for Vascularization of the Gastrointestinal Tract. *Nature* **1998**, *393*, 591–594, doi:10.1038/31261.
46. Zhang, Q.; Guo, R.; Schwarz, E.M.; Boyce, B.F.; Xing, L. TNF Inhibits Production of Stromal Cell-Derived Factor 1 by Bone Stromal Cells and Increases Osteoclast Precursor Mobilization from Bone Marrow to Peripheral Blood. *Arthritis Res Ther* **2008**, *10*, R37, doi:10.1186/ar2391.
47. Ratajczak, M.Z.; Serwin, K.; Schneider, G. Innate Immunity Derived Factors as External Modulators of the CXCL12 - CXCR4 Axis and Their Role in Stem Cell Homing and Mobilization. *Theranostics* **2013**, *3*, 3–10, doi:10.7150/thno.4621.
48. Sato, S.; Sakurai, T.; Ogasawara, J.; Takahashi, M.; Izawa, T.; Imaizumi, K.; Taniguchi, N.; Ohno, H.; Kizaki, T. A Circadian Clock Gene, Rev-Erbα, Modulates the Inflammatory Function of Macrophages through the Negative Regulation of Ccl2 Expression. *J. Immunol.* **2014**, *192*, 407–417, doi:10.4049/jimmunol.1301982.
49. Spengler, M.L.; Kuropatwinski, K.K.; Comas, M.; Gasparian, A.V.; Fedtsova, N.; Gleiberman, A.S.; Gitlin, I.I.; Artemicheva, N.M.; Deluca, K.A.; Gudkov, A.V.; et al. Core Circadian Protein CLOCK Is a Positive Regulator of NF-κB–Mediated Transcription. *Proc. Natl. Acad. Sci. U.S.A.* **2012**, *109*, E2457–E2465, doi:10.1073/pnas.1206274109.
50. Adachi, A.; Honda, T.; Dainichi, T.; Egawa, G.; Yamamoto, Y.; Nomura, T.; Nakajima, S.; Otsuka, A.; Maekawa, M.; Mano, N.; et al. Prolonged High-Intensity Exercise Induces Fluctuating Immune Responses to Herpes Simplex Virus Infection via Glucocorticoids. *J. Allergy Clin. Immunol.* **2021**, *148*, 1575-1588.e7, doi:10.1016/j.jaci.2021.04.028.
51. Kwon, M.-S.; Seo, Y.-J.; Choi, S.-M.; Won, M.-H.; Lee, J.-K.; Park, S.-H.; Jung, J.-S.; Sim, Y.-B.; Suh, H.-W. The Time-Dependent Effect of Lipopolysaccharide on Kainic Acid-Induced Neuronal Death in Hippocampal CA3 Region: Possible Involvement of Cytokines via Glucocorticoid. *Neuroscience* **2010**, *165*, 1333–1344, doi:10.1016/j.neuroscience.2009.11.060.
52. Zhang, R.; Lahens, N.F.; Ballance, H.I.; Hughes, M.E.; Hogenesch, J.B. A Circadian Gene Expression Atlas in Mammals: Implications for Biology and Medicine. *Proc. Natl. Acad. Sci. U.S.A.* **2014**, *111*, 16219–16224, doi:10.1073/pnas.1408886111.
53. Okudaira, N.; Akimoto, M.; Susa, T.; Akimoto, M.; Hisaki, H.; Iizuka, M.; Okinaga, H.; Almunia, J.A.; Ogiso, N.; Okazaki, T.; et al. Accumulation of Senescent Cells in the Adrenal Gland Induces Hypersecretion of Corticosterone via IL1β Secretion. *Aging Cell* **2024**, *23*, e14206, doi:10.1111/acel.14206.
54. Minaduola, M.; Aili, A.; Bao, Y.; Peng, Z.; Ge, Q.; Jin, R. The Circadian Clock Sets a Spatial–Temporal Window for Recent Thymic Emigrants. *Immunol Cell Biol* **2022**, *100*, 731–741, doi:10.1111/imcb.12582.
55. Arjona, A.; Sarkar, D.K. Circadian Oscillations of Clock Genes, Cytolytic Factors, and Cytokines in Rat NK Cells. *J. Immunol.* **2005**, *174*, 7618–7624, doi:10.4049/jimmunol.174.12.7618.
56. Zhen, Y.; Wang, Y.; He, F.; Chen, Y.; Hu, L.; Ge, L.; Wang, Y.; Wei, W.; Rahmat, A.; Loor, J.J.; et al. Homeostatic Crosstalk among Gut Microbiome, Hypothalamic and Hepatic Circadian Clock Oscillations, Immunity and Metabolism in Response to Different Light–Dark Cycles: A Multiomics Study. *J Pineal Res* **2023**, *75*, e12892, doi:10.1111/jpi.12892.
57. Pariollaud, M.; Ibrahim, L.H.; Irizarry, E.; Mello, R.M.; Chan, A.B.; Altman, B.J.; Shaw, R.J.; Bollong, M.J.; Wiseman, R.L.; Lamia, K.A. Circadian Disruption Enhances HSF1 Signaling and Tumorigenesis in *Kras* -Driven Lung Cancer. *Sci. Adv.* **2022**, *8*, eabo1123, doi:10.1126/sciadv.abo1123.
58. Zhao, Y.; Liu, M.; Chan, X.Y.; Tan, S.Y.; Subramaniam, S.; Fan, Y.; Loh, E.; Chang, K.T.E.; Tan, T.C.; Chen, Q. Uncovering the Mystery of Opposite Circadian Rhythms between Mouse and Human Leukocytes in Humanized Mice. *Blood* **2017**, *130*, 1995–2005, doi:10.1182/blood-2017-04-778779.

 doi:10.20944/preprints202606.0096.v1

59. Noh, J.Y.; Han, H.W.; Kim, D.M.; Giles, E.D.; Farnell, Y.Z.; Wright, G.A.; Sun, Y. Innate Immunity in Peripheral Tissues Is Differentially Impaired under Normal and Endotoxic Conditions in Aging. *Front. Immunol.* **2024**, *15*, 1357444, doi:10.3389/fimmu.2024.1357444.
60. Kumari, R.; Verma, V.; Singaravel, M. Simulated Chronic Jet Lag Affects the Structural and Functional Complexity of Hippocampal Neurons in Mice. *Neuroscience* **2024**, *543*, 1–12, doi:10.1016/j.neuroscience.2024.01.026.
61. Franceschi, C.; Bonafè, M.; Valensin, S.; Olivieri, F.; De Luca, M.; Ottaviani, E.; De Benedictis, G. Inflamm-Aging: An Evolutionary Perspective on Immunosenescence. *Ann N Y Acad Sci* **2000**, *908*, 244–254, doi:10.1111/j.1749-6632.2000.tb06651.x.
62. Wu, Y.; Zhang, S.; Chen, H.; He, X.; Yang, G. Circadian Clock: A Regulator of Immunity in Autoimmune Diseases. *Immun Inflamm Dis* **2025**, *13*, e70246, doi:10.1002/iid3.70246.
63. Lin, G.-J.; Huang, S.-H.; Chen, S.-J.; Wang, C.-H.; Chang, D.-M.; Sytwu, H.-K. Modulation by Melatonin of the Pathogenesis of Inflammatory Autoimmune Diseases. *Int J Mol Sci* **2013**, *14*, 11742–11766, doi:10.3390/ijms140611742.
64. Amir, M.; Chaudhari, S.; Wang, R.; Campbell, S.; Mosure, S.A.; Chopp, L.B.; Lu, Q.; Shang, J.; Pelletier, O.B.; He, Y.; et al. REV-ERBα Regulates TH17 Cell Development and Autoimmunity. *Cell Rep* **2018**, *25*, 3733-3749.e8, doi:10.1016/j.celrep.2018.11.101.
65. Du, J.; Zhang, F.; Chen, M.; Xiao, Y.; Zhang, L.; Dong, L.; Dong, D.; Wu, B. Jujuboside A Ameliorates Cognitive Deficiency in Delirium through Promoting Hippocampal E4BP4 in Mice. *J Pharm Pharmacol* **2023**, *75*, 886–897, doi:10.1093/jpp/rgad057.
66. Hergenhan, S.; Holtkamp, S.; Scheiermann, C. Molecular Interactions Between Components of the Circadian Clock and the Immune System. *J Mol Biol* **2020**, *432*, 3700–3713, doi:10.1016/j.jmb.2019.12.044.
67. Curtis, A.M.; Fagundes, C.T.; Yang, G.; Palsson-McDermott, E.M.; Wochal, P.; McGettrick, A.F.; Foley, N.H.; Early, J.O.; Chen, L.; Zhang, H.; et al. Circadian Control of Innate Immunity in Macrophages by miR-155 Targeting Bmal1. *Proc. Natl. Acad. Sci. U.S.A.* **2015**, *112*, 7231–7236, doi:10.1073/pnas.1501327112.
68. Cavadini, G.; Petrzilka, S.; Kohler, P.; Jud, C.; Tobler, I.; Birchler, T.; Fontana, A. TNF-α Suppresses the Expression of Clock Genes by Interfering with E-Box-Mediated Transcription. *Proc. Natl. Acad. Sci. U.S.A.* **2007**, *104*, 12843–12848, doi:10.1073/pnas.0701466104.
69. Pariollaud, M.; Gibbs, J.E.; Hopwood, T.W.; Brown, S.; Begley, N.; Vonslow, R.; Poolman, T.; Guo, B.; Saer, B.; Jones, D.H.; et al. Circadian Clock Component REV-ERBα Controls Homeostatic Regulation of Pulmonary Inflammation. *J Clin Invest* **2018**, *128*, 2281–2296, doi:10.1172/JCI93910.
70. Zhou, J.; Wang, H.; Ouyang, Q. Mathematical Modeling of Viral Infection and the Immune Response Controlled by the Circadian Clock. *J Biol Phys* **2024**, *50*, 197–214, doi:10.1007/s10867-024-09655-5.
71. Fajgenbaum, D.C.; June, C.H. Cytokine Storm. *N Engl J Med* **2020**, *383*, 2255–2273, doi:10.1056/NEJMra2026131.
72. Okin, D.; Medzhitov, R. Evolution of Inflammatory Diseases. *Curr Biol* **2012**, *22*, R733–R740, doi:10.1016/j.cub.2012.07.029.
73. Germain, R.N. Maintaining System Homeostasis: The Third Law of Newtonian Immunology. *Nat Immunol* **2012**, *13*, 902–906, doi:10.1038/ni.2404.
74. Ince, L.M.; Weber, J.; Scheiermann, C. Control of Leukocyte Trafficking by Stress-Associated Hormones. *Front. Immunol.* **2019**, *9*, 3143, doi:10.3389/fimmu.2018.03143.